

# GOTHIC-3D APPLICABILITY TO HYDROGEN COMBUSTION ANALYSIS

JUNG-JAE LEE\*, JIN-YONG LEE, GOON-CHERL PARK<sup>1</sup>, BYUNG-CHUL LEE<sup>2</sup>,  
HOJONG YOO, HYEONG-TAEK KIM and SEUNG-JONG OH<sup>3</sup>

<sup>1</sup>Seoul National University

San56-1, Sillim-dong, Kwanak-gu, Seoul, Korea, 151-742

<sup>2</sup>Future & Challenge Technology, Co., Ltd.

San4-1 Bongchon7-dong, Kwanak-gu, Seoul, Korea, 151-818

<sup>3</sup>Korea Hydro & Nuclear Power Co., Ltd.

103-16, Munji-dong, Yuseong-gu, Daejeon, Korea, 305-380

\*Corresponding author. E-mail : doublej2@snu.ac.kr

*Received August 16, 2004*

*Accepted for Publication December 29, 2004*

---

Severe accidents in nuclear power plants can cause hydrogen-generating chemical reactions, which create the danger of hydrogen combustion and thus threaten containment integrity. For containment analyses, a three-dimensional mechanistic code, GOTHIC-3D has been applied near source compartments to predict whether or not highly reactive gas mixtures can form during an accident with the hydrogen mitigation system working. To assess the code applicability to hydrogen combustion analysis, this paper presents the numerical calculation results of GOTHIC-3D for various hydrogen combustion experiments, including FLAME, LSVCTF, and SNU-2D. In this study, a technical base for the modeling of large- and small-scale facilities was introduced through sensitivity studies on cell size and burn modeling parameters. Use of a turbulent burn option of the eddy dissipation concept enabled scale-free applications. Lowering the burn parameter values for the flame thickness and the burn temperature limit resulted in a larger flame velocity. When applied to hydrogen combustion analysis, this study revealed that the GOTHIC-3D code is generally able to predict the combustion phenomena with its default burn modeling parameters for large-scale facilities. However, the code needs further modifications of its burn modeling parameters to be applied to either small-scale facilities or extremely fast transients.

---

**KEYWORDS** : GOTHIC-3D, Hydrogen Combustion, Burn Model, Flame Velocity, Containment, Nuclear Power Plant

---

## 1. INTRODUCTION

Severe accidents in a nuclear power plants (NPP) can generate substantial amounts of hydrogen via the chemical reactions between the zirconium cladding and the hot water vapor, as well as by the core-concrete interactions after a lower head failure of the vessel. Such generated hydrogen can be transported into the compartments of the containment building, and it has the potential to threaten containment integrity by over-pressurization via hydrogen combustion, as by deflagration or detonation. Moreover, even local hydrogen burning, which is not a threat to global containment integrity, may also threaten the survivability of safety-related equipment.

Because of such a scenario, a three-dimensional mechanistic code, GOTHIC-3D, has been applied near source compartments to predict whether or not highly reactive gas mixtures can be formed during an accident with the hydrogen mitigation system (HMS) working.

However, the direct application of GOTHIC-3D to NPP containment without a discrimination of the characteristics of each concerned compartment would cause considerable uncertainties regarding the results of analyses.

Therefore, in this study, several sets of sensitivity studies were addressed to identify the influences of GOTHIC-3D modeling on hydrogen combustion phenomena, especially on flame propagation, under various conditions of size and geometry. We intended to ultimately derive the most applicable modeling parameters for the conditions of each relevant compartment. To meet this objective, we have selected three experiments and compared the results of our numerical analyses to those of the experiments. The selected experiments were Flame Acceleration Measurements and Experiments (FLAME) [1], Large-Scale Vented Combustion Tests Facility Experiments (LSVCTF) [2], and Seoul National University 2D Experiments (SNU-2D) [3].

**Table 1.** Initial and Boundary Conditions in Experiments

Experiment	Initial and Boundary Conditions							
	Temperature	Pressure	Gas Mixture	H <sub>2</sub> Conc.	Area of Vent or Exit	Obstacle	Ignition Point	Wall Materials
FLAME	25°C	84.1kPa	H <sub>2</sub> /Air	12.3%	4.46m <sup>2</sup>	No	Center of Left Plate	Reinforced Concrete
LSVCTF	27°C	100kPa	H <sub>2</sub> /Air	11.0%	1.12m <sup>2</sup>	No	Center of Volume	Steel Plate
SNU-2D	25°C	101kPa	H <sub>2</sub> /Air	12.0%	0.012m <sup>2</sup>	Yes	Center of Upper Wall	Acrylic Plate

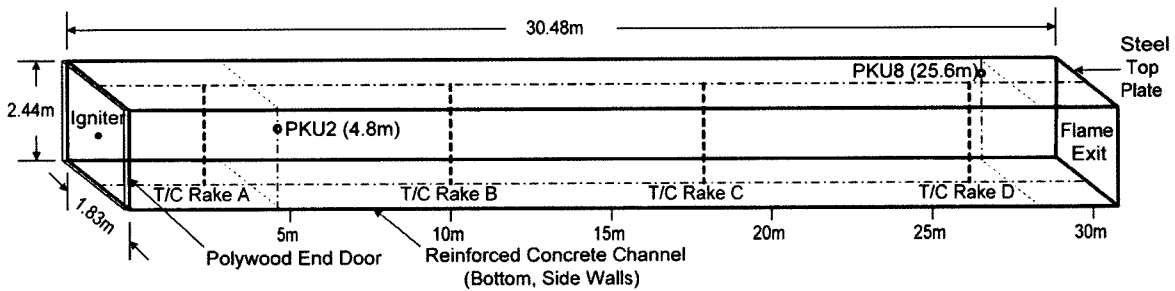


Fig. 1. FLAME Facility and Locations of Measurements

## 2. EXPERIMENTS CONSIDERED

### 2.1 FLAME Experiments

Table 1 shows the conditions of experiments selected for this study. The FLAME experiment involves a large horizontal rectangular channel made of heavily-reinforced concrete, with dimensions of 30.48 m × 2.44 m × 1.83 m (100 ft × 8 ft × 6 ft), as shown in Figure 1. The apparatus considered here was designed and built for the U.S. Nuclear Regulatory Commission. It is a half-scaled model of the upper plenum volume found in ice condenser PWR containments. In the FLAME experiments, twenty-nine sets of test were executed, during which the hydrogen mole fraction was varied from 12 % to 30 %.

In this study, a geometrically simple test case (Test F-10 in the series of experiments), in which there was no obstacle or transverse venting, was selected as a representative case. This was because GOTHIC-3D has hardly been applied to hydrogen combustion analysis and because there are some geometry modeling limitations with the GOTHIC code. Moreover, we kept in mind that the initial hydrogen concentrations should be near 14.2 % of volume, because this condition makes hydrogen control impossible in the Advanced Power Reactor 1400 MW (APR1400). The hydrogen concentration in the selected test case was 12.3 %.

### 2.2 LSVCTF Experiments

The LSVCTF experiments are large-scale combustion tests in a rectangular facility with dimensions of 10 m × 4

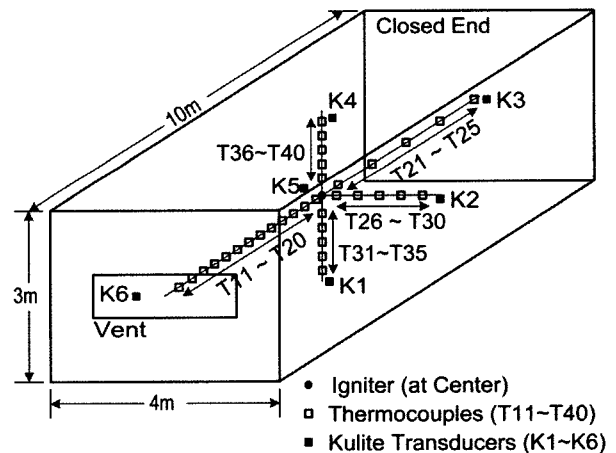


Fig. 2. LSVCTF Facility and Locations of Measurements

m × 3 m. A schematic of the facility is shown in Figure 2. The wall is composed of a 1.25 cm-thick steel plate and a 1 m-thick concrete layer outside the steel plate. Two roller-mounted movable end walls are provided to open up the vessel for internal modifications or to move-in bulky experimental equipment when needed. An igniter is located at the center of the volume and a vent is located on the one of end walls to guarantee the flame flows. The vent area can be changed by removing or replacing the appropriate number of panels. Temperatures and pressures are locally measured to provide data regarding flame

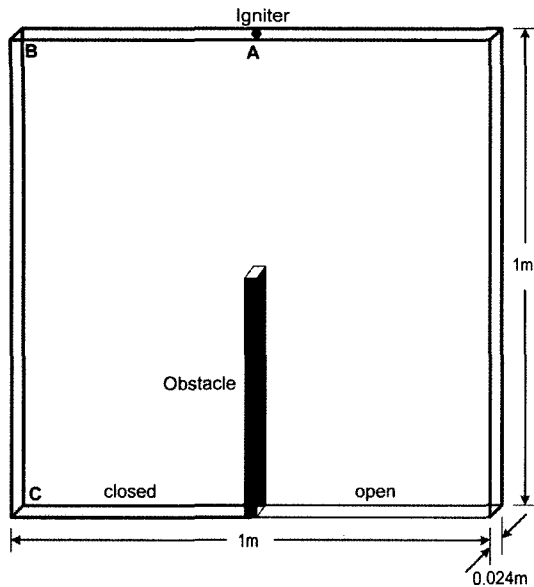


Fig. 3. SNU-2D Combustion Chamber

propagations. In the considered experiments, the initial hydrogen concentration was varied from 8.5 % to 12 %, in accordance with each test, and the flame velocity, pressure, and hydrogen concentrations were measured.

For GOTHIC simulation, a test case was selected in which the initial hydrogen concentration was 11.0 % and the area of the vent at the left wall was 1.12 m<sup>2</sup>. This case had a relatively similar initial hydrogen concentration compared to the aforementioned relevant value of 14.2 %.

### 2.3 SNU-2D Experiments

In the SNU-2D experiments, the combustion chamber has an upright planar shape with dimensions of 1 m × 1 m × 0.024 m. Figure 3 shows a schematic of the SNU-2D combustion chamber, which is composed of a transparent acrylic plate and a sealing rubber plate supported by an aluminum frame. Hydrogen gas is injected into the combustion chamber through a needle valve equipped at the back of the plate and the initiation of combustion is achieved with an igniter equipped in the chamber. Six sets of tests were executed in the SNU-2D experiments. Effects of the existence of an obstacle, of igniter position (points A, B and C in Figure 3), and of bottom opening condition were tested. Hydrogen concentrations of 10 %, 12 %, and 12.3 % were used in the experiments. For the present study, the case using a 12 % concentration of hydrogen was selected.

## 3. GOTHIC-3D ANALYSES

### 3.1 General Description of GOTHIC-3D Code [4]

GOTHIC-3D is a general-purpose thermal hydraulics computer program for design, licensing, safety, and

operating analyses of NPP. Applications of GOTHIC-3D to analyses include hydrogen combustion phenomena in containment, as well as overall thermal hydraulic phenomena, such as high-energy line breaks and containment heat-up calculations.

### 3.2 Hydrogen Burn Models

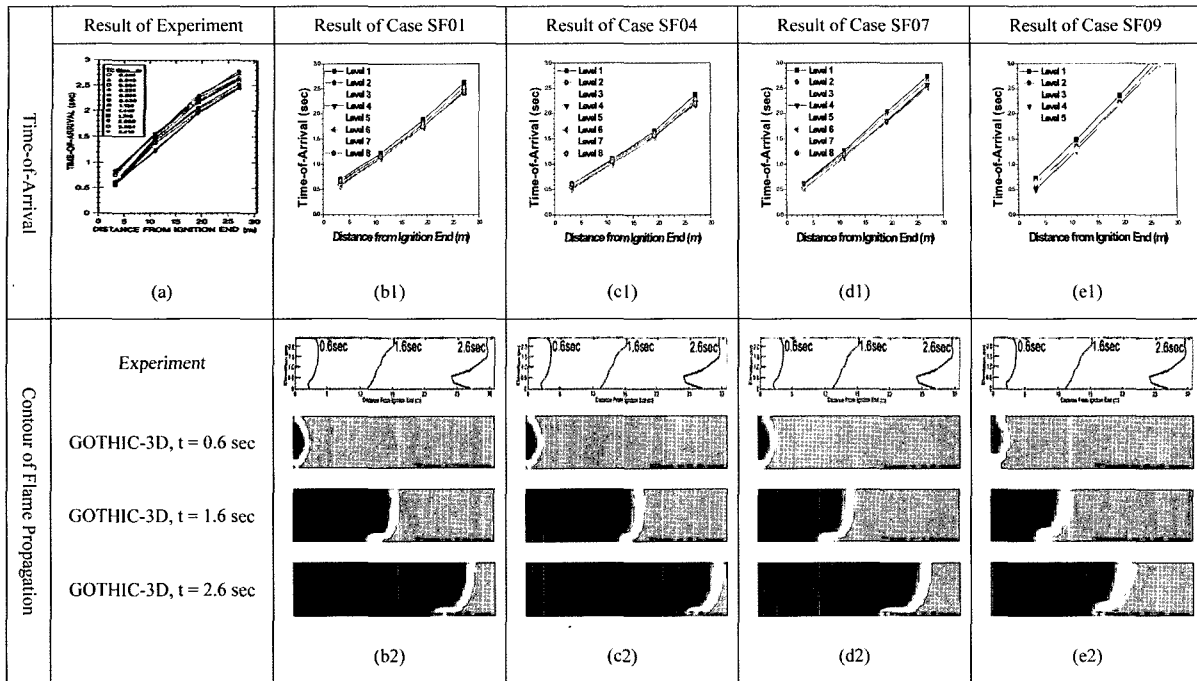
The GOTHIC-3D code includes hydrogen burn models for lumped parameter volumes and subdivided volumes. The lumped parameter burn models are almost identical to the burn model described in HECTR [5] and CONTAIN [6] codes, which consist of the discrete burn model and the continuous burn model. The discrete burn model burns a specified fraction of existing hydrogen within a volume when specified gas mixture criteria are met. The continuous burn model continuously burns hydrogen flowing into a volume from a junction. In the discrete burn model, the flame speed is calculated using built-in functions of the mole fractions for steam, oxygen, and hydrogen. The time required to burn hydrogen within a volume is calculated by dividing the burn length by the flame speed.

The mechanistic burn model is applicable to subdivided volumes. When this option is specified, burning of hydrogen requires that the mole fraction limits be satisfied. If the mole fraction limits are satisfied, then the combustion of hydrogen is continuously calculated. The combustion rate of hydrogen is determined from the maximum of the laminar and turbulent combustion rates. Laminar combustion is preset to zero and is not calculated unless the effective temperature for combustion exceeds the user specified lower temperature limit. The laminar burn model is given by *Lewis and von Elbe* [7]. The turbulent burn model has two options: the eddy dissipation concept of *Magnussen and Hjertager* [8] and the turbulent flame speed based concept of *Damköhler* [9]. In the model for the turbulent reaction rate, two empirically based limitations are imposed. The first is referred to as cold quenching and the second condition is referred to as high-turbulence flame quenching.

## 4. RESULTS

### 4.1 Simulation of FLAME

Figure 4 illustrates the experimental data of time-of-arrival and flame propagation produced by four or more thermocouple rakes, pressure transducers, and additional thermocouples. Lines in time-of-arrival data shown in Figure 4(a) indicate the flame velocity at each level undergoing variation as flame propagates. Flame propagation in experiment is shown in the upper part of Figures 4(b2), 4(c2), 4(d2), and 4(e2). Test results indicate the flame propagation toward the exit of channel finished in 3 seconds and weak flame acceleration occurred. Because of the buoyancy force, the flame propagation showed concave shapes with slower velocities at the lower part



\* Captures of experimental data were quoted from M.P. Sherman et al.

Fig. 4. Time-of-Arrival Data and Contours of Flame Propagation in FLAME Chamber, GOTHIC-3D

of the channel. Figures 4(b) to 4(e) show the results of GOTHIC-3D calculations for some representative cases described in Table 2.

Comparison of Figure 4(b) and Figure 4(e) provides the cell-size dependency in the GOTHIC-3D model. Firstly, case SF01, with default values of burn parameters, shows good agreement both in scale of time-of-arrival and in propagation shape of flame front, compared with the experimental results, though flame acceleration was not found in case SF01, while the experimental data shows it was present. However when the length of the cell dimension is increased by about a factor of 2, as in case SF09, the flame propagation becomes much slower than that of case SF01. Because the overall flame velocity is slow, the buoyancy effect becomes relatively more dominant, so the gradient in the flame surface becomes larger.

The dependency of turbulent burn options on flame propagation was investigated. While most cases presented in this paper used the eddy dissipation (EDIS) model, the flame speed (FSPD) model was used in cases SF04 and SF05. Figure 4(c) shows the results of the calculation for case SF04 using the FSPD model. The difference between case SF04 and case SF05 is that case SF04 used default burn parameters, while case SF05 used 100°C as  $T_{lim}$ . The effect of  $\delta_f$  was not considered, because if the FSPD model is selected, the flame front thickness parameter  $\delta_f$  is canceled out in equations. The FSPD model resulted in somewhat faster values of flame propagation, as illustrated in Figure 4(c). In case SF05, additional calculation, we

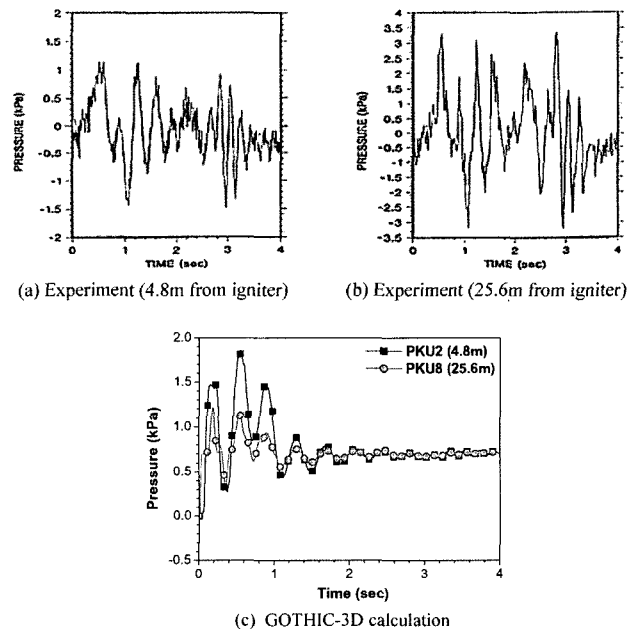


Fig. 5. Comparison of Pressure History in FLAME Facility

found that the flame speed was much faster than those in case SF04 because lower burn temperature limit was used in case SF05. The resultant effect was also similar to that of the comparison between cases SF01 and SF03, in which the EDIS model was used.

Table 2. Calculation Matrix

Experiment	Simulation No.	Modeling Features			
		Cell Size (m <sup>3</sup> )	Turb. Option	T <sub>lim</sub> (°C)	δ <sub>r</sub> (m)
FLAME	SF01 <sup>a)</sup>	0.0283 <sup>b)</sup>	EDIS	175	0.05
	SF02	0.0283	EDIS	175	0.01
	SF03	0.0283	EDIS	100	0.05
	SF04	0.0283	FSPD	175	Default <sup>e)</sup>
	SF05	0.0283	FSPD	100	Default
	SF06	0.0238	EDIS	150	0.005
	SF07	0.0238	EDIS	175	0.005
	SF08	0.0238	EDIS	190	0.005
	SF09	0.2265 <sup>c)</sup>	EDIS	175	0.05
	SF10	0.2265	FSPD	175	Default
LSVCTF	SL01 <sup>a)</sup>	0.1013	EDIS	175	0.05
	SL02	0.0156	EDIS	175	0.05
	SL03	0.1013	FSPD	175	Default
	SL04	0.1013	EDIS	150	0.05
	SL05	0.1013	EDIS	100	0.05
	SL06	0.1013	EDIS	175	0.03
	SL07	0.1013	EDIS	175	0.01
	SL08	0.1013	EDIS	175	0.005
	SL09	0.1013	EDIS	180	0.005
	SL10	0.1013	EDIS	150	0.005
	SL11	0.1013	EDIS	130	0.005
SNU-2D	SS01 <sup>a)</sup>	1.64x10 <sup>-5d)</sup>	EDIS	175	0.05
	SS02	1.64x10 <sup>-5</sup>	EDIS	175	0.03
	SS03	1.64x10 <sup>-5</sup>	EDIS	175	0.01
	SS04	1.64x10 <sup>-5</sup>	EDIS	175	0.001
	SS05	1.64x10 <sup>-5</sup>	EDIS	100	0.05
	SS06	1.64x10 <sup>-5</sup>	EDIS	100	0.001
	SS07	1.64x10 <sup>-5</sup>	FSPD	175	Default
	SS08	1.64x10 <sup>-5</sup>	FSPD	100	Default

a) Base case using default parameters for each experiment

b) 0.0283 m<sup>3</sup> = 1.0 ft<sup>3</sup>c) 0.2265 m<sup>3</sup> = 8.0 ft<sup>3</sup>d) 1.64x10<sup>-5</sup> m<sup>3</sup> = 1.0 in<sup>3</sup>e) Default value of δ<sub>r</sub> for FSPD option = 0.05

Figure 4(d) illustrates the results when δ<sub>r</sub> is set to 0.005 m. Since the empirical value of laminar flame thickness is about 10<sup>-4</sup> m and that of turbulent flame is 10 to 100 times thicker [10], we considered 0.005 m as an approximate value of δ<sub>r</sub>. In this case, there is little difference in flame propagation as compared to case SF01 using default values. However, the time-of-arrival data improved in viewpoint of flame acceleration as flame approaches.

From the parametric effect calculations, we found the dependencies of modeling such as cell size, turbulent burn models, and two burn parameters on GOTHIC-3D results. The best agreements were found in case SF01 and case SF07 in viewpoint of flame propagation. These cases use the EDIS model as a turbulent burn option and in turbulent burn option, the former case used the default values of T<sub>lim</sub> and δ<sub>r</sub> while the latter case did default value of T<sub>lim</sub> and modified value with a factor of 0.1 for δ<sub>r</sub>. Case SF01 showed a better result in time of arrival at the exit

while case SF07 showed a better result in flame acceleration. However, the dependency of the cell size in subdivided volume was found to be a critical factor when modeling a facility. In the comparison of results for cell size, a better agreement was found in cases using smaller cells, i.e., 0.3 m-based modeling rather than 0.6 m-based modeling.

The pressure histories during the transient were also compared. Figure 5 shows the pressure histories at two points in the FLAME channel for case SF01. As shown in the figure, the peak pressure in the channel was 3.4 kPa in the experiment and this value was not critical, because it showed extremely low variations. *Sherman et al.* [1] reported that up to the time that the deflagration exited the channel, the period of the oscillations was about 300 msec. In the GOTHIC-3D calculation, we found a similar peak pressure and period of oscillations. However, we also found some limitations in predicting the pressure histories. In the results of the GOTHIC-3D calculation,

the peak pressure was slightly lower than that of the experiment and a larger peak was found at a point near the ignition end. Moreover, the pressure oscillation was highly attenuated and transversal pressure wave propagation was not visible. These discrepancies in the pressure histories could have resulted from too small a simulation of the ambient volume, which was due to the roughly distributed in the three dimensional modeling. Detailed sensitivity analysis for the cell dimensions will be further investigated in the next stage of this study.

### 4.2 Simulation of LSVCTF

In the LSVCTF experiments, there was a combustion duration before the start of flame propagation. However, the code could not simulate this physical phenomenon. Thus, the location of the first thermocouple in each direction from the igniter was set as the reference point for the comparison of time-of-arrival data in both the experiments and code simulations. Figure 6 shows the comparative results of the representative cases. As seen in the figure, no significant difference could be found in any case; however, there were slight distinctions in accordance with the modeling parameters.

As shown in Table 2, the effect of the cell size can be found by comparing case SL01, which is the default case, to case SL02. The difference between the two cases is the volume of the three-dimensionally subdivided cells. In the default case, the volume was uniformly subdivided into 0.1013 m<sup>3</sup>-cells, while 0.0156 m<sup>3</sup>-cells for case SL02. Comparison of both cases did not show significant difference for the results of flame propagation toward each direction. However for case SL02, with about seven times as many cells as those in case SL01, much larger and uneconomical computational efforts were required. Accordingly, the three-dimensional model of case SL01 was considered as the basic three-dimensional modeling

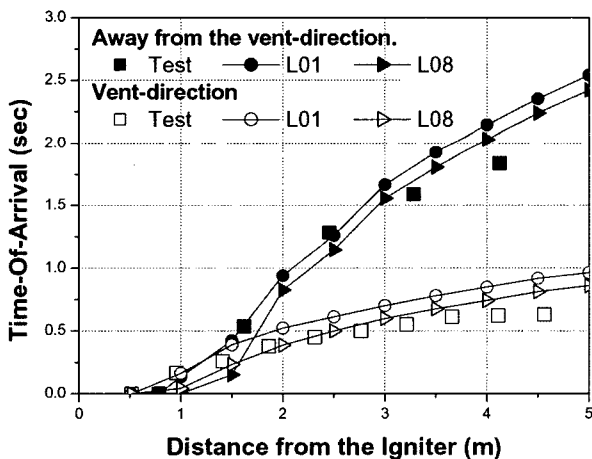
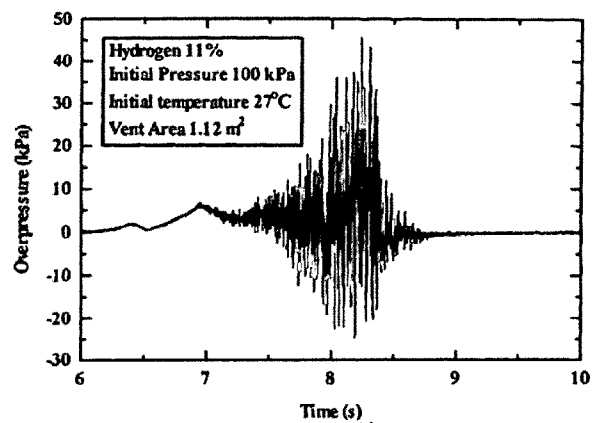


Fig. 6. Time-of-Arrival Data for Flame Propagation in LSVCTF Chamber, GOthic-3D

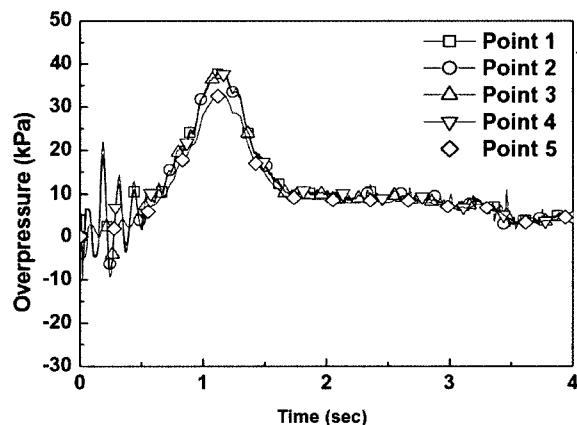
for LSVCTF simulations.

A comparison for turbulence options was made between EDIS and FSPD using default values for other modeling parameters. This comparison corresponds to the one made between case SL01 and case SL03 in Table 2. The results of both directions in the chamber show little differences in time-of-arrival data and show few differences when compared to the experimental data.

Using the three-dimensional model for case SL01 and the EDIS turbulence option, the sensitivity for parametric effects was examined. As shown in Table 2, several attempts to find the best agreement with the experimental data were successful. We found that, in general, the results of the code calculations approached the experimental values when decreasing the values of  $T_{lim}$  and/or  $\delta_f$  were used; however,  $T_{lim}$  did affect the results less significantly than  $\delta_f$ . As additional considerations, the empirical flame front thickness reported by Williams [10] was used to model the problems in cases SL08 to SL11. These cases showed



(a) Experiment (Loesel Sitar et al.)



(b) GOthic-3D calculation  
(Points 1 to 5 correspond to K5, K1, K4, K3 and K6 in Fig. 2, respectively.)

Fig. 7. Comparison of Pressure History in LSVCTF Facility

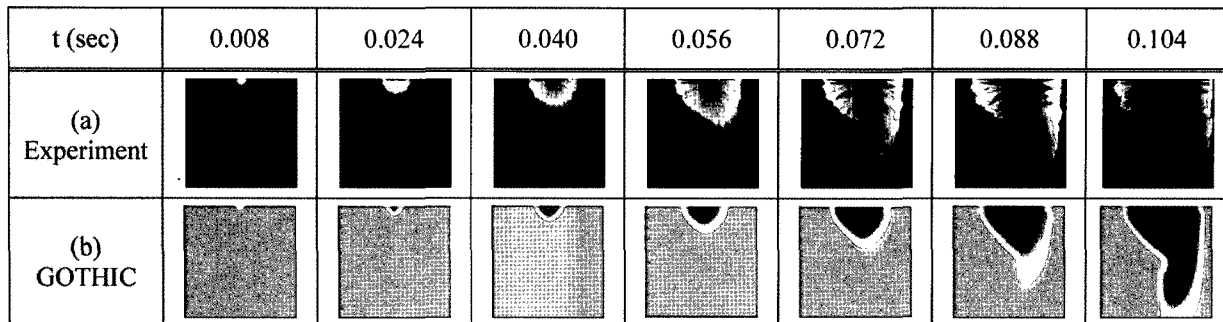


Fig. 8. Comparison of the Results Between SNU-2D Experiment and GOTHIC-3D Simulation (case SS06)

Table 3. Optimal Modeling Parameters for Each Experiment

Experiment	Volume (m <sup>3</sup> )	Number of Cells	Modeling Parameters		
			Basic Length of a Cell (m) <sup>a)</sup>	$\delta_r$ (m)	$T_{im}$ (°C)
FLAME	135.92	5,280	0.3048	0.005	175
LSVCTF	120.0	1,323	0.45	0.005	175
SNU-2D	0.025	1,681	0.025	0.001	100

a) This value reveals the representative length of a cell three-dimensionally subdivided volume in GOTHIC-3D analysis

somewhat better agreements with the experimental data. However, the results did not vary significantly and the most agreeable values for those variables were determined.

From various sensitivity studies, the most suitable values of the modeling parameters for the LSVCTF experiments were found for case SL08, which uses the same three-dimensional model as case SL01 and the EDIS turbulence option with the default values of 175°C, and 0.005 m for  $T_{im}$  and  $\delta_r$ , respectively. As with the FLAME experiments, some limitations were found; however, the peak pressure was reasonably well predicted, as shown in Figure 7. The difference in time for two graphs was caused by the combustion duration during the experiment, as described above.

#### 4.3 Simulation of SNU-2D

The SNU-2D experiment is a very small-scaled test to be applied to GOTHIC-3D calculation. For this experiment, the cell size dependency was not examined, but the volume was two-dimensionally subdivided, with similar lengths of chamber thickness of about 0.024 m. In this analysis, the code with the default model or a model in which one parameter was modified, could not accurately predict the fast transient as measured in the experiments. Accordingly, parametric effect simulations were performed with various combinations of  $T_{im}$  and  $\delta_r$ .

In most simulations addressed in Table 2, the times-

of-arrival of the flame at the opening region of the chamber were generally within 1 second after ignition, while the measured data was about 0.1 second. Figure 8 illustrates the final, most acceptable result. Figure 8(a) shows high-speed CCD camera images from the test, while Figure 8(b) illustrates the GOTHIC-3D simulation of case SS06. As shown in the figure, the GOTHIC-3D prediction shows good agreement with experimental data in which  $\delta_r$  and  $T_{im}$  are 0.001 m and 100°C, respectively.

## 5. SUMMARY AND DISCUSSION

From the results described above, it can be said that with a smaller cell size, a larger flame propagation velocity is generated and that if the length of the cell approaches  $\delta_r$ , the flame propagation velocity becomes larger as decreasing  $\delta_r$ . For the large-scale facilities of FLAME and LSVCTF, similar results were found for both EDIS and FSPD turbulence models; for the small-scale facility, SNU-2D, with only the EDIS option, faster flame propagations were simulated. The resultant optimal modeling parameters for each experiment are shown in Table 3.

For FLAME experiments, the GOTHIC-3D simulations did not clearly show the flame acceleration phenomena; the variation of  $\delta_r$  did not cause significant effects on the

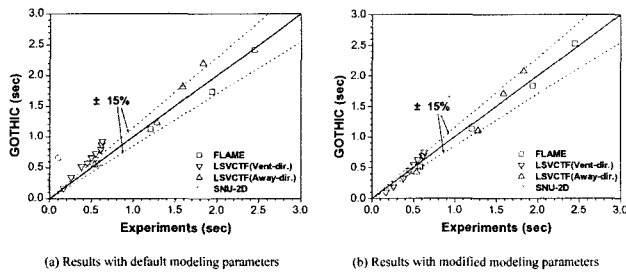


Fig. 9. Comparison of Time-of-Arrival Data Between GOTHIC-3D Simulations and Experimental Results

results, while the variation of  $T_{lim}$  caused more significant effects with a fixed flame thickness. In the LSVCTF simulations, no significant effects were caused by either parameter. Through the sensitivity analyses for LSVCTF experiments, the most agreeable result for the flame propagation was found with exactly the same modeling values as those used in the FLAME simulation. However for the small-scale facility of the SNU-2D experiment, the results from using a large-scale facility were no longer valid. The best set of modeling parameters existed in much smaller ranges for both parameters than those resulted in large-scale facility simulations.

Figure 9 summarizes the results for all the simulations. It compares the time-of-arrival data from the GOTHIC-3D calculations to those from experiments. Figure 9(a) shows the results when using the default parameters of  $\delta_f$  and  $T_{lim}$ , while Figure 9(b) shows the best set of modeling parameters for each simulation. It should be noted that the set of data in Figure 9(b) was not obtained with the same modeling parameters. The figure shows the results with the most agreeable modeling parameters for each test. A comparison of the two figures revealed no significant differences for large-scale facilities, and this shows that the default modeling values of GOTHIC-3D can be used to analyze combustion phenomena in large-scale facilities. However, good agreement of results between the experiments and the GOTHIC-3D simulations were seen when modifying the parameters, especially in a small-scale facility or in a region where the time-of-arrival is very short.

## 6. CONCLUSIONS

The applicability of GOTHIC-3D to hydrogen combustion analysis was investigated. Three hydrogen combustion experiments, in which the initial hydrogen concentrations were similar to that of the APR1400 issued level, were selected for simulations. Characteristics of the GOTHIC-3D burn models and their applicability can be summarized as follows. For large-scale facilities, the default modeling parameters could be used with

appropriately distributed cells. However, slightly better results are obtained with reduced flame thickness with a factor of 0.1. On the other hand, the modeling parameters must be corrected to simulate fast transients, especially in very small-scale facilities, because GOTHIC-3D does not predict such situations well when using the default modeling parameters.

In conclusion, it was shown that GOTHIC-3D has conditional applicability to combustion analysis. Flame propagations were relatively well predicted by the code, with some correction of burn modeling parameters. However, in viewpoint of pressure history, the observations in this study show that further investigations should be performed to determine the general criteria by which the code can be applied to combustion analysis. Such work could be carried out by using an approach similar to the one used in this study, i.e., by comparing calculation results to experimental results for other tests performed in the same large-scale facilities considered in this study.

## REFERENCES

- [1] M.P. Sherman, S.R. Tiezen and W.B. Benedick, "The Effect of Obstacles and Transverse Venting on Flame Acceleration and Transition to Detonation for Hydrogen-Air Mixtures at Large Scale," NUREG/CR-5275, Sandia National Laboratories, Albuquerque, pp. 1-49 (1989).
- [2] J. Loesel Sitar, G.W. Koroll, W.A. Dewit, E.M. Bowles, J. Harding, C.L. Sabanski and R.K. Kumar, "The Large-Scale Vented Combustion Test Facility at AECL-WL: Description and Preliminary Test Results," AECL-11762, AECL Whiteshell Laboratories, Pinawa, pp. 219-233 (1997).
- [3] J.Y. Lee, J.J. Lee, G.C. Park and S.H. Chung, "Experimental Assessment of GOTHIC Code for Local Hydrogen Combustion Analysis," *Proceedings of PSAM7 - Probabilistic Safety Assessment and Management*, June 14-18, 2004, Berlin (2004).
- [4] T.L. George, L.E. Wiles, S.W. Claybrook, C.L. Wheeler, J.D. McElroy and L. Agee, GOTHIC Containment Analysis Package Technical Manual – Version 6.1b, NAI 8907-06 Rev. 11, pp. 10.1-10.13, NAI, Washington (2001).
- [5] S.E. Dingman, A.L. Camp, C.C. Wong, D.B. King and R.D. Gasser, *HECTR Version 1.5 User's Manual*, NUREG/CR-4507, Sandia National Laboratories, Albuquerque, NM (1986).
- [6] K.K. Murata and D.C. Williams, Code Manual for CONTAIN 2.0 : A computer code for nuclear reactor containment analysis, NUREG/CR-6533, USNRC, Washington D.C. (1997).
- [7] B. Lewis and G. von Elbe, *Combustion, Flames and Explosions of Gases*, Chapter VI, Academic Press, Inc., New York (1961).
- [8] B.F. Magnussen, and B.H. Hjertager, "On Mathematical Modeling of Turbulent Combustion with Special Emphasis on Soot Formation and Combustion," *Proceedings of 16th International Symposium on Combustion*, pp. 719-729, The Combustion Institute (1976).
- [9] G. Damköhler, *Zeit. Electrochem*, **46**, pp. 601 (1949).
- [10] F.A. Williams, *Combustion Theory*, **2nd ed.**, pp. 130-136, 373-440, Addison-Wesley Publishing Company, Princeton Univ. (1996).